



IMPACT OF INTERFACE GEOMETRY ON THE SEISMIC RESPONSE OF FREESTANDING STRUCTURES

M.K. Saifullah⁽¹⁾, A. Barnard⁽²⁾, C.E. Wittich⁽³⁾

⁽¹⁾ Graduate Research Assistant, Department of Civil and Environmental Engineering, University of Nebraska-Lincoln, USA, khalidsaif@huskers.unl.edu

⁽²⁾ Undergraduate Research Assistant, Department of Civil and Environmental Engineering, University of Nebraska-Lincoln, USA, abarnardx@huskers.unl.edu

⁽³⁾ Assistant Professor, Department of Civil and Environmental Engineering, University of Nebraska-Lincoln, USA, cwittich@unl.edu

Abstract

Freestanding structures constitute a wide range of structures ranging from classical multi-drum columns in historic structures to modern rocking wall systems and electrical transformers. This class of structures includes critical systems to support the post-earthquake functionality of buildings, irreplaceable cultural heritage structures, and precariously balanced rock systems (PBRs) which are necessary for accurate seismic hazard characterization at long return periods. Therefore, accurate prediction of the seismic response of freestanding structures is imperative. Despite the seeming simplicity of freestanding structures, the seismic response is known to be highly nonlinear with respect to geometry and extremely sensitive to small changes in the geometry, orientation, and ground excitation. Owing to this complexity, geometrically-simplified models are often utilized in predictive studies, with substantial simplification occurring at the base of the freestanding structure (the interface). In an effort to better predict the performance of freestanding structures under earthquake loads, this study aims to evaluate the impact of the interface geometry on the overturning rates for freestanding structures. A preliminary numerical study on naturally occurring freestanding precariously balanced rocks was conducted to briefly learn about the impact of footprint geometry. This was followed by an experimental investigation, in which 3D printed models of various prototype freestanding structures incorporating a range of interface/footprint geometries were used in a scaled shake table testing campaign. The critical geometric parameters in two-dimensions (rocking radius and critical angle) were held constant throughout the testing to isolate the impact of the interface shape. A large number of near-fault ground motions representing a range of intensities were used as excitation in the shake table tests. The experimental results are compared with analytical analyses on simplified 2D model to elucidate the conservativeness of results for overturning behavior. The rate of overturning was assessed probabilistically through seismic fragility curves and is shown to be fairly consistent for the majority of the interface shapes tested, though key differences emerged for shapes with sharp angular irregularities in the interface.

Keywords: Freestanding Structures; Rocking; Precariously Balanced Rocks; Seismic Hazard; Distinct Element Method



1. Introduction

The term “freestanding structures” refers to structures that are free to slide (translate), rock (rotate), slide-rock (translate-rotate) and potentially overturn under certain conditions. These structures include man-made structures such as multi-drum columns, statue-pedestal systems, electrical transformers, sensitive mechanical and electrical equipment, as well as naturally occurring structures such as precariously balanced rocks. While rocking behavior may be beneficial for some structures as it creates an isolation-like effect, it may be highly detrimental for some other structures. Moreover, a complete collapse or the overturning of these structures under earthquake excitation could result in total loss or irreparable damage of the structure. Even if overturning is avoided, rocking may be undesirable for these structures, particularly sensitive equipment, which may see high accelerations upon each impact. Previous studies on freestanding structures indicate that the response of these structures is very sensitive to certain geometric, excitation, and interface parameters that introduce a great deal of uncertainty in their response. One of the critical interface parameters that may dictate the response is the geometry at the interface (or contact), which is the focus of this study.

Although early on, Milne [1] and Kirkpatrick [2] studied the uplifting and overturning of freestanding structures in an effort to estimate the peak acceleration of ground motion (to quantify earthquake intensity), Housner’s study [3] on inverted pendulum structures is typically considered the foundational study which stimulated the interest of researchers in rocking structures. Later, others expanded this concept by introducing other freestanding structure modes such as slide, slide-rocking, free-flight or jump etc. [4, 5]. Since then, a number of studies have been conducted on freestanding structures, in two and three-dimensions with varying level of complexity (e.g., single and multiblock problems with pure rocking and/or other modes) and involving analytical and/or numerical and/or experimental work [e.g., 6, 7, 8, 9, 10].

In terms of geometrical complexity, Purvance [11] and Purvance et al. [12] established overturning fragilities for asymmetric and symmetric blocks. Wittich and Hutchinson [13, 14], through a series of shake table tests, explored the effect of geometrical complexity/asymmetry on the seismic response of freestanding structures. With particular reference to the basal interface, Mathey et al. [15] noticed that non-negligible out-of-plane motion exists even in cases of apparent in-plane initial conditions, while doing free oscillation tests on a large slender steel block with standard manufacturing quality. This observation compelled them to study the geometrical defects at the interface by employing statistical tools on a large number of numerical simulations and ultimately reached a conclusion that the model with geometrical defects is more vulnerable to rocking and overturning than the model, which is free from defects. Similarly, Wittich and Hutchinson [16] analytically studied the effect of interface defects on freestanding structures. Their study indicates that small interface defects or asperities can lead to large variation in the seismic response of these structures. Taking this problem from another perspective, Bachmann [17] extended the classical rocking problem to account for an extended flat base and curved wedges at the interface to study its efficacy as a seismic mitigation strategy. Along a similar theme, Makris and Black [18] investigated the seismic stability of rigid electrical equipment supported on extended flat base foundations and concluded that even a small amount of base protrusion can substantially reduce the uplift. In addition to the geometrical complexity at the interface, a number of other studies have been conducted that analyzed the impact of interface material. ElGawdy et al. used concrete, timber, steel, and rubber as interface materials to study their effect on the free rocking response of blocks of different aspect ratios. With rubber dissipating energy much faster than other interface materials, their study shows that free rocking response is greatly influenced by the interface materials and imperfections [19]. A recent numerical study by Saifullah and Wittich [20] on freestanding statue-pedestal systems resting on soil similarly concluded that interface material in multi-block systems can have a substantial impact on the response modes and the overturning rate of these systems.

While previous research has shown that geometric asperities and material variations at the interface of freestanding structures can result in significant variations in the seismic response, a detailed treatment of the contact shape has not yet been presented. To this end, numerical, experimental and analytical studies are presented herein to understand the impact of three-dimensional contact or interface geometry. The numerical work acts as a preliminary study to qualitatively analyze the difference in response brought about by random



geometrical changes at the footprint by employing naturally occurring freestanding structures, precariously balanced rocks (PBRs). These PBRs are critical for seismic hazard and are geometrically complex freestanding structures. In order to more systematically study this issue, a scaled shake table testing campaign was conducted, incorporating a range of footprint shapes with increasing numbers of potential rocking edges. Finally, for direct comparison with experimental work, theoretical analyses with an equivalent rectangular 2D model are presented. For consistency, the results are analyzed in terms of seismic fragility curves, which rely on two principal and critical ground motion parameters, peak ground acceleration (PGA) and the peak ground velocity normalized by the peak ground acceleration (PGV/PGA).

2. Review of Rigid Body Rocking

The classical rigid body rocking problem, as first studied by Housner [3], modeled a freestanding structure as a simplified 2D projection of a rectangular rocking block, symmetric about its center of mass (Fig. 1). Once excited into rocking, the block rotates about alternating centers of rocking, O and O' , assumedly making perfectly plastic impacts such that free flight does not occur. This model also assumes sufficient friction at the contact interface to prevent sliding. Three geometric parameters govern the block's rocking behavior: the moment of inertia about the center of mass, I , the radius from the center of rocking to the center of mass, $R = \sqrt{h^2 + b^2}$, and the angle between that radius and the vertical, α . The center of mass, M , is located at a width b and height h from the center of rotation. Once excited, the block rocks about either corner through an angle, θ , and potentially overturn or collapse.

Eq. (1) presents a comprehensive, analytically derived equation of motion for the 2D block shown in Fig. 1 under horizontal ground acceleration, \ddot{x}_g , which is a function of the block's geometry and the amplitude of ground motion. Although the equation represents the theoretical rocking response mode, it is highly nonlinear with respect to geometry. Additionally, the function is piecewise with respect to the direction of rocking due to the alternating centers of rotation. As per the signum function, the last term, $(\theta)mRg\sin(\alpha - |\theta|)$ is positive when θ is positive, and negative when θ is negative. Thus, even with the model fully described, its equation of motion is difficult to implement, and a unique, closed-form solution is unattainable for most ground motions. The coefficient of restitution, e , presented in Eq. (2), is the derived measure of elasticity of the block's impacts, accounting for energy loss during rocking. Moreover, the assumption holds that energy dissipation is lumped at a point (O or O') and occurs instantaneously at the time of impact. Consequently, the classical rocking model is limited in its application to more complex contact and interface geometries and materials. Like the equation of motion, this coefficient is also non-linear with respect to geometry.

$$(I + mR^2)\ddot{\theta} = mR\cos(\alpha - |\theta|)\ddot{x}_g - \text{sign}(\theta)mRg\sin(\alpha - |\theta|) \quad (1)$$

$$e = \frac{\dot{\theta}_{\text{before}}}{\dot{\theta}_{\text{after}}} = 1 - \frac{3}{2}\sin^2 \alpha \quad (2)$$

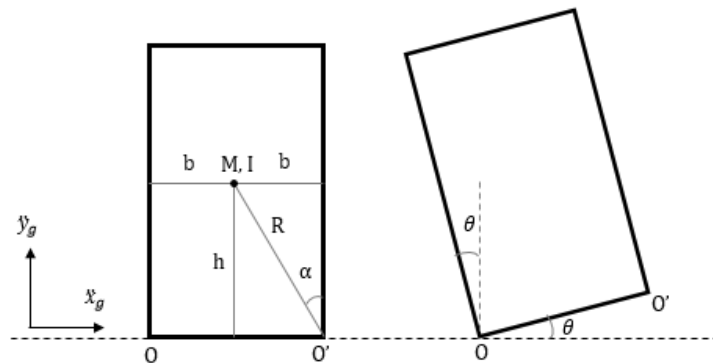


Fig. 1 - 2D block rocking through angle θ



3. Numerical Case Study

A numerical case study involving precariously balanced rocks (PBRs) is conducted to assess the impact of interface geometry on the PBRs. A highly asymmetric PBR, with a height of about 6.234 ft (190 cm), is employed in this study (Fig. 2a). As these simulations are used as preliminary analyses to study the impact of interface geometry, overturning fragility analyses are conducted by using the actual PBR contact interface as well as the same PBR with a base area increased by 10%. In the remainder of this paper, the former is referred to as Model 1, while the latter is referred to as Model 2. The methodology adopted for modeling of PBRs, the historical ground motions employed for the analyses, and the results in the form of fragilities are discussed in the following sub-sections.

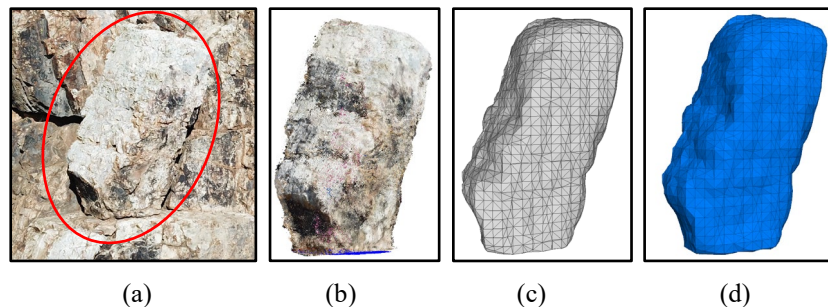


Fig. 2 - Precariously Balanced Rock a) Original b) Point cloud c) 3D surface mesh d) 3D volumetric mesh

3.1 Methodology

The PBRs are modeled by using three-dimensional point clouds generated through Structure-from-Motion (SfM, Fig. 2b). As SfM derived point clouds are unitless/dimensionless, the SfM was scaled by using terrestrial or ground-based lidar (also known as 3D laser scanning). As shown in the snapshots, the point cloud is merely a group of x,y,z coordinates corresponding to the surface of the PBR within the line of sight of the camera (SfM) or the scanner (lidar). The point clouds are converted into a 3D watertight surface mesh by using a Poisson Surface Reconstruction (PSR) algorithm (Fig. 2c) [21], as implemented in Meshlab [22]. PSR is chosen as it is known to conveniently handle sharp gradients by considering the entire point cloud at once and can successfully handle complex geometries, as evident from a number of previous studies [e.g. 19, 23, 24].

3D surface meshes of the PBRs are imported into a distinct element program, 3DEC [25], which was developed based on Cundall's pioneering efforts on distinct element method [26]. Given the nature of the problem being studied, the distinct element approach is preferred over other techniques (such as finite element method) as it allows large rotation and complete detachment in addition to its versatility in contact detection. The 3D surface meshes are converted into actual volumetric models by utilizing a material density of 162 lb/ft³ (2600 kg/m³) to reflect rock-like material (Fig. 2d). A ground block and surrounding rock is modeled within the program with the same material to reflect the pedestal to which the excitation is applied. As the geometrical interfaces in a distinct element program are characterized by joint normal and shear stiffnesses, a typical stiffness value of 1 GPa/m is used for this purpose. The rock and the ground block are treated as rigid blocks with the deformation concentrated only at the interface, which not only optimizes the calculation time but also fairly approximates the real behavior of the rocky masses.

3.2 Input ground motions

The ground motion records for the numerical simulations are predominantly near-fault records taken from PEER NGA-West2 database [27]. The only exceptions are the 2015 Gorkha-Nepal earthquake records, which are retrieved from Center for Engineering Strong Motion Data (CESMD) [28]. The two orthogonal horizontal



components of the ground motion are combined to obtain a single representative intensity measure that is independent of the orientation. The intensity measures RotD₅₀ PGV/PGA and RotD₅₀ PGA are calculated using the procedure presented by Boore [29]. RotD₅₀ is the median amplitude or 50th percentile of response spectra over all non-redundant rotations of a given pair of horizontal components of ground motion [27]. The median amplitude of the spectra at period of 0 s corresponds to RotD₅₀ PGA. As the numerical analyses are to be performed under horizontal bidirectional excitation, all the as-recorded ground motion time series are rotated to North and East to align the input time series along two orthogonal directions of the model. A total of 70 bidirectional records, covering a range of RotD₅₀ PGV/PGA values, are selected for the analyses. Each horizontal component of the selected records is normalized by RotD₅₀ PGA and multiplied with a range of scale factors (i.e. 0.2 g to 1.0 g) to obtain 9 intensity levels of PGA, which, in turn, results in 630 analyses for each PBR model. 5% damped orientation independent RotD₅₀ elastic spectra are shown in Fig. 3a. With the two horizontal components of each ground motion shown with two distinct colors, Fig. 3b presents all the scaled ground motions used in the numerical study. However, it is noted that the number of earthquake records available decreases significantly at high RotD₅₀ PGV/PGA ratios.

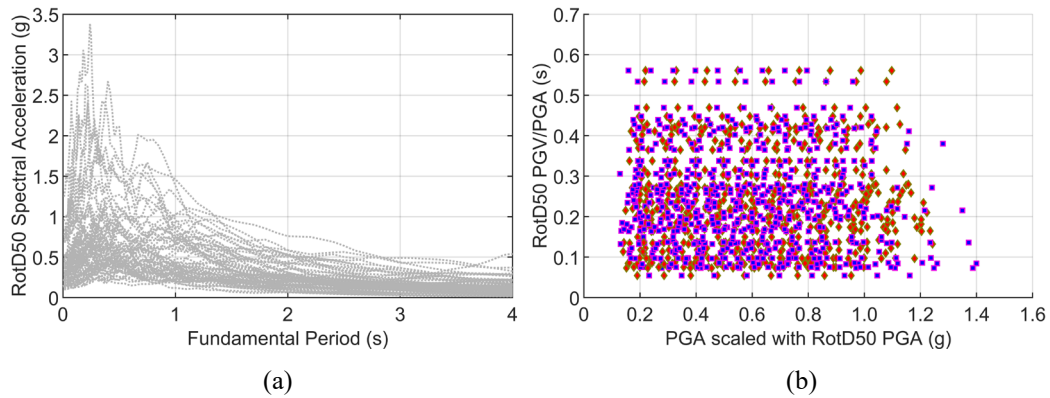


Fig. 3 – Ground motion records a) 5% damped elastic spectra b) RotD₅₀ PGA vs RotD₅₀ PGV/PGA

3.3 Analyses and results

Seismic fragility analyses are performed by using the numerical outcomes from the PBRs analyses. Due to the dichotomous nature of the outcome (i.e. overturning or no overturning), a bivariate logistic regression is adopted to study the combined relation of RotD₅₀ PGA and RotD₅₀ PGV/PGA with the probability of overturning. In other words, it is a way to estimate the probability of overturning with vector-valued ground motion intensity measures. A bivariate logistic regression is similar to univariate logistic regression as it deals with binary outcomes considering two covariates (or independent variables) instead of one covariate. The logit function or log-odds can be expressed in the form of Eq. (3), while, the probabilities of overturning given the two covariates, can be calculated using Eq. (4):

$$\text{logit} \left[P \left\{ O \mid \text{PGA} = x_1, \frac{\text{PGV}}{\text{PGA}} = x_2 \right\} \right] = \beta_0 + \beta_1 x_1 + \beta_2 x_2 \quad (3)$$

$$P \left(O \mid \text{PGA} = x_1, \frac{\text{PGV}}{\text{PGA}} = x_2 \right) = \frac{e^{\beta_0 + \beta_1 x_1 + \beta_2 x_2}}{1 + e^{\beta_0 + \beta_1 x_1 + \beta_2 x_2}} \quad (4)$$

where $P(O)$ represents probability of overturning, x_1 and x_2 are the covariates, and β_0 , β_1 , β_2 are regression coefficients. As the distribution associated with the logistic regression is a binomial distribution, the maximization of the likelihood function is necessary to estimate the unknown regression coefficients. The likelihood function, L , in its compact form is presented in Eq. (5):



$$L(\beta_0, \beta_1, \beta_2) = \prod_{i=1}^n P(x_i)^{y^i} (1 - P(x_i))^{1-y^i} \quad (5)$$

where y^i is the binomial distribution variable, which equals unity if overturning occurs and is null otherwise. $P(x_i)$ is the probability of overturning given the two intensity measures PGA and PGV/PGA. Usually, the maximum likelihood estimates are found by employing the log-likelihood of this equation, differentiated with respect to the parameters $(\beta_0, \beta_1, \beta_2)$. The derivatives are then set equal to zero and solved numerically since the closed-form solution is not possible.

The probabilities of overturning can then be obtained at the intensity levels of interest, which are transformed into a fragility surface by plotting with the corresponding intensity measures. These fragility surfaces provides valuable information regarding the (probabilistic) vulnerability of the structure at various vector-valued intensities. This robust and consistent approach is used throughout this study to compare the fragilities of different structures, which is vital to understand the impact of interface geometries. The fragility surfaces for the two PBR models developed using the aforementioned procedure are shown in Fig. 4. Except the lowest level (i.e., 16%), the two fragility surfaces intersect each other at all the probability levels considered (Fig. 4c). With a 10% increase in the contact area at the base of the PBR (Model 2), the same probability of overturning is achieved at a lower PGV/PGA value when compared with Model 1. Specifically, at a PGA of 0.2 g, Model 2 has a 95% probability of overturning at a PGV/PGA of 0.58 s, while Model 1 has a 95% probability of overturning at a PGV/PGA of 0.70 s. Given the substantial differences observed in the probabilistic overturning for these two freestanding structures, further investigation is warranted to study the effect of the interface shape on the rate of overturning, which is explained in the next section.

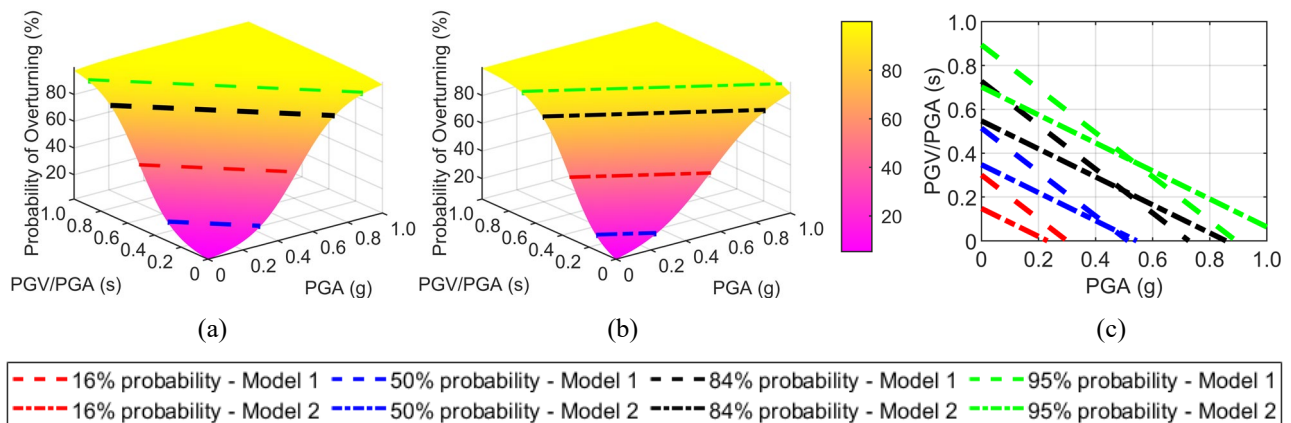


Fig. 4 – Fragility Analyses with a) Fragility surface for Model 1 b) Fragility Surface for Model 2 c) Cross-sections at different probability levels

4. Experimental Program

Though a few studies have been conducted on geometrically complex freestanding structures, the knowledge in this domain is still scarce. With the overturning treated as the main response variable, this experimental program aims to unlock the impact of the complexity of the interface geometry on the seismic response of freestanding structures. To this end, 3D printed models incorporating different geometrical shapes are subjected to a series of shake table tests to quantify the overturning fragilities for geometrical variations at the base of the structures. The different response modes, such as rocking, twisting, sliding, rock-twist, rock sliding, have also been qualitatively studied during the process. However, given that the main focus of this paper is the overturning response, only overturning is comprehensively analyzed in this paper.



4.1 Ground motions

A subset of 50 recorded ground motions, covering a wide range of PGV/PGA ratios, is selected from the aforementioned historical earthquakes (see Section 3.2). The elastic response spectra of this subset of ground motions are shown in Fig 5a. It is noted that these spectra are not orientation independent, as was shown in Fig. 3), since the experimental program used a uni-axial shake table. As PGA is also included in the fragility analysis, these 50 ground motions are scaled to different PGA levels (~ 0.2 g to 0.85 g) to obtain an adequate distribution of PGA values. The resulting 200 ground motions along with the PGA achieved on the shake-table are presented in Fig 5b.

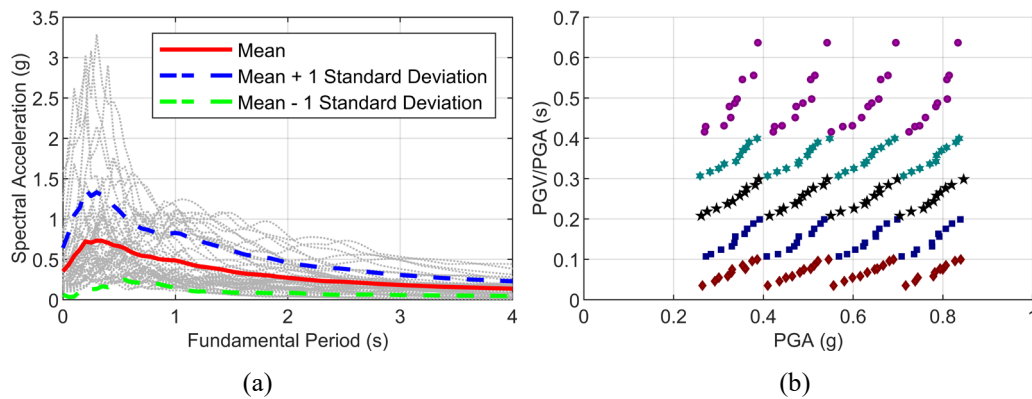


Fig. 5 – All ground motions with plots showing a) 5% damped elastic response spectra b) PGV/PGA and the PGA achieved with the shake table – different colors depict different bins

4.2 Experimental protocol and instrumentation

4.2.1 Design of Structural Models

The design of the 3D structural models is conducted such that their 2D projection is consistent across all geometries and consistent with the rectangular block studied by Housner [3]. Models with footprints of 5 different geometrical shapes are designed to study the influence of interface geometry on the overturning demand. Since rocking behavior is predominantly dictated by the block's geometry, particularly the slenderness, α , and the rocking radius, R , these two-dimensional parameters are kept fairly constant for each structural model. Each model consists of a single 2 in x 2 in x 10 in (5.08 cm x 5.08 cm x 25.4 cm) slender, hollow rectangular tower bolted interchangeably with one hollow base part with a unique footprint geometry. The different footprint geometries are shown in Fig. 6a, while the relevant geometrical parameters are listed in Table 1. A square base is intended to be a close approximation to the analytical or theoretical solution, while a circular base is an extremely contrasting case. While the circular model involves roughly a point contact in the rocking mode due to the absence of straight rocking edge, the hexagonal and octagonal footprints allow for the investigation of the impact arising from the transition between square and circular shapes. Out of all the models, the triangular footprint is distinct in the sense that it rocks about a corner/point in one direction, while rocks on an edge when the rocking direction is reversed, even though the rocking plane is same. With the exception of the square model, out-of-plane motion is expected in all the models, which also allows to study the additional response modes which may bring about the overturning (though not a focus of this study). It is noted that the horizontal footprint dimensions are selected to be slightly larger than the base projection of the hollow rectangular superstructure, which aids in the easy manipulation of the geometry without compromising the value of critical parameters. The test models are 3D printed with a rigid material to constrain the contribution of flexibility towards response.



4.2.2 Experimental Setup and Testing Protocol

The testing protocol is conducted using an APS 400 shaker with an APS 145 amplifier operated in a horizontal uniaxial shake table mode, which can take a maximum payload of 50 lb (23 kg) and offers a peak-to-peak relative stroke capability of 6.25 in (15.875 cm). Owing to the smooth surface of the table, sandpaper is affixed to the table to increase the friction between the geometrical interface of the model and the table to minimize sliding. The acceleration atop the shake table is monitored through an accelerometer rigidly placed on the shake table platen. To visually capture both the in-plane and out-of-plane motion of the models, two cameras placed parallel and perpendicular to the direction of excitation are used. Additional arrangements are made to protect the model and the accelerometer from damage by utilizing lightweight foam pieces as shown in Fig. 6b. A measuring tape is also affixed to roughly quantify the movement and change in position of the model and is further supplemented by a grid marked on the sandpaper. Each of the 5 models are subjected to the aforementioned 200 ground motions for a total of 1000 ground motion tests. Different response modes such as rocking, sliding, and twisting are manually recorded by visual observations. In cases of ambiguity, the high-frame rate video recordings from the cameras are used to differentiate between rocking and rock-sliding. Following each test, the model position is reset to a preselected grid point near the center of the table to maintain consistency between tests.

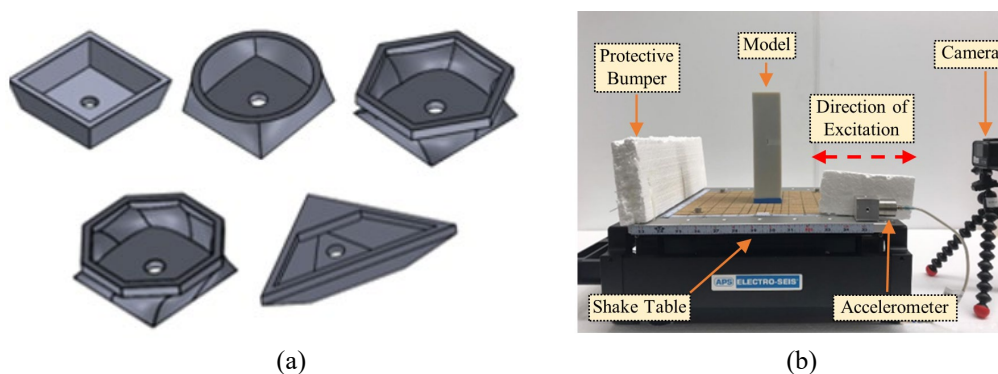


Fig. 6 – Test setup a) Footprint geometries b) Instrumentation

Table 1 - Geometrical shapes and the relevant parameters

| Shape of Base | R [in (cm)] | α [°] |
|---------------|---------------|--------------|
| Square | 5.34 (13.563) | 12.98 |
| Hexagon | 5.40 (13.716) | 12.94 |
| Octagon | 5.40 (13.716) | 12.96 |
| Circle | 5.38 (12.990) | 12.99 |
| Triangle | 5.34 (13.563) | 12.79 |

4.3 Results

Similar to the numerical results, the experimental results are presented in the form of fragility surfaces. These seismic fragilities are calculated in the same manner as those previously presented. To compare the fragilities of different models, cross-sections are taken at the 50% and the 95% probability overturning levels, as shown in Figs. 7 and 8. In general, there is a stark difference between the fragility surface of the triangular model (Fig. 7e) and the rest of the geometries. This vivid distinction is likely arising due to the asymmetry of the triangular model's footprint (i.e., rocking about a point in one direction and rocking about an edge in the



opposite direction). It was observed that uplift about a point, rather than edge, results in instability where the model can quickly change direction or mode. This contributes significantly to the out-of-plane motion and more combination modes such as rock-twist, rock-slide as compared to other models, which typically uplifted and rocked about edges.

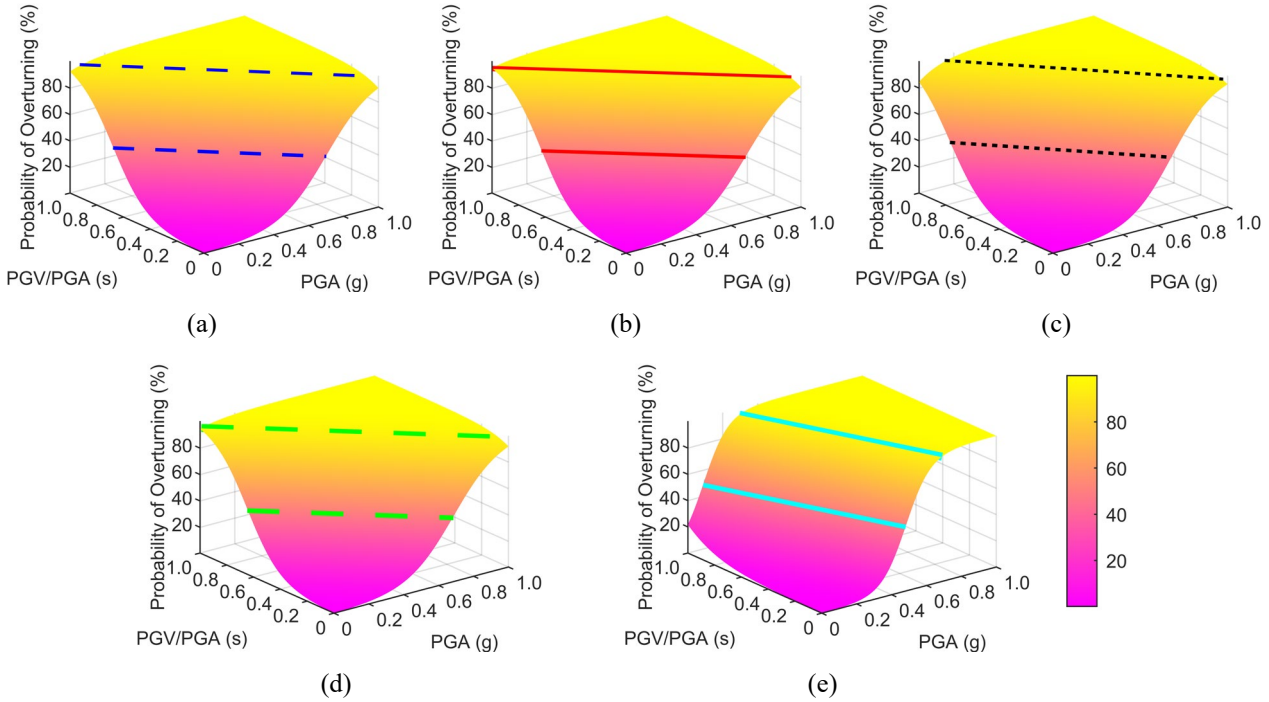


Fig. 7 – Fragility surfaces for interfaces with geometry a) Square b) Circle c) Hexagon d) Octagon e) Triangle

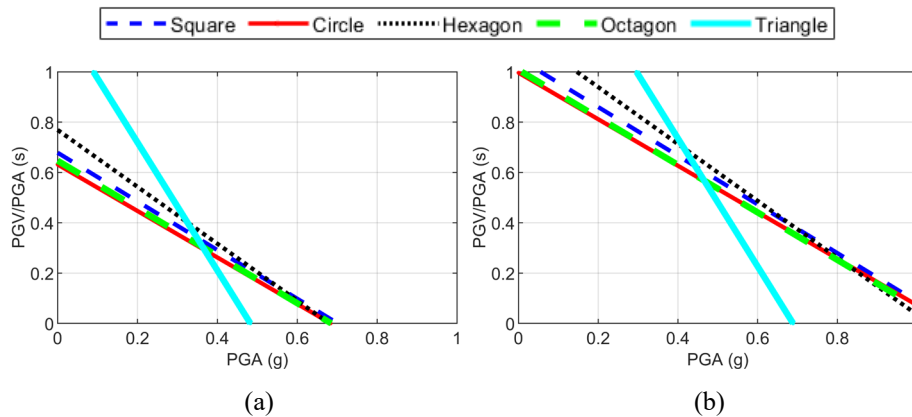


Fig. 8 - Cross-sections of fragility surfaces at probability of overturning a) 50% b) 95%

At all probability levels, the overturning rate is similar for the circular and octagonal models which is likely due to the high number of edges of the octagon, which allows the response to approximate the wobble of the circle. The probability of overturning for the square and hexagonal base models, though not exactly coinciding with circular and octagonal curves, is still relatively similar to them. For example, at a PGA of 0.2 g, all the models except the triangle have a 50% probability of overturning for PGV/PGA between approximately 0.45 s and 0.55 s. On the other hand, the triangular model achieves a similar rate of overturning



at a PGV/PGA of nearly 0.75 s. In addition, it is noted that the triangular model is also much more sensitive to PGA as compared to PGV/PGA. Due to a much higher slope of the 2D cross-section (Fig 8d) at both probability levels, a large percentage of overturning can be achieved at lower levels of PGA. This stark deviation in terms of the intensity measures indicates that the response of the triangular model is not classical rocking behavior, and the PGA and PGV/PGA intensity measures may not be sufficient to reflect the overturning behavior of rocking blocks with such sharp angles at the interface.

4.4 Analytical Comparison

The purpose of keeping the rocking radius, R , and critical angle of rotation, α , consistent in the physical test models was not only to allow for a robust comparison between responses from different geometrical footprints but was also intended to compare and contrast responses obtained from these experimental models and the theoretical 2D response. The theoretical response is based on the theory briefly mentioned in Section 2 of this paper. The 2D dimensions of the model are 2 in x 10 in (5.08 cm x 25.4 cm - 1:5 aspect ratio), which are analogous to the 3D dimensions of the physical models. Though R and α values for all models are nearly the same, the exact R and α values of 5.34 in (13.563 cm) and 12.98° are used to replicate the response of a square model. The equation of motion (Eq. 1) was numerically integrated for all ground motions in a 4th-5th order Runge-Kutta time-stepping scheme in MATLAB [30], where the angular velocity was reduced according to the restitution relationship of Eq. (2) at each identified impact event. The results of these analytical simulations were analyzed in a similar fashion to the previous sections as 3D fragility surface (see Fig. 9a). Comparison plots between the analytical and experimental results are shown at two probability levels of overturning (i.e., 50% and 95%) – Fig. 9b and 9c. In general, the analytical model predicts that the structure would overturn at lower intensity ground motions compared to the tested models indicating that the theoretical model is likely conservative. This is true for all of the interface shapes tested, including the square base which closely replicates the theoretical conditions. The difference can be attributed to the theoretical model's restriction to pure rocking motion, inability to capture out-of-plane motion, and treatment of contact. Specifically, the equations presented in Section 2 assume perfect point impacts, while the actual specimens impacted and pivoted about a finite edge or point.

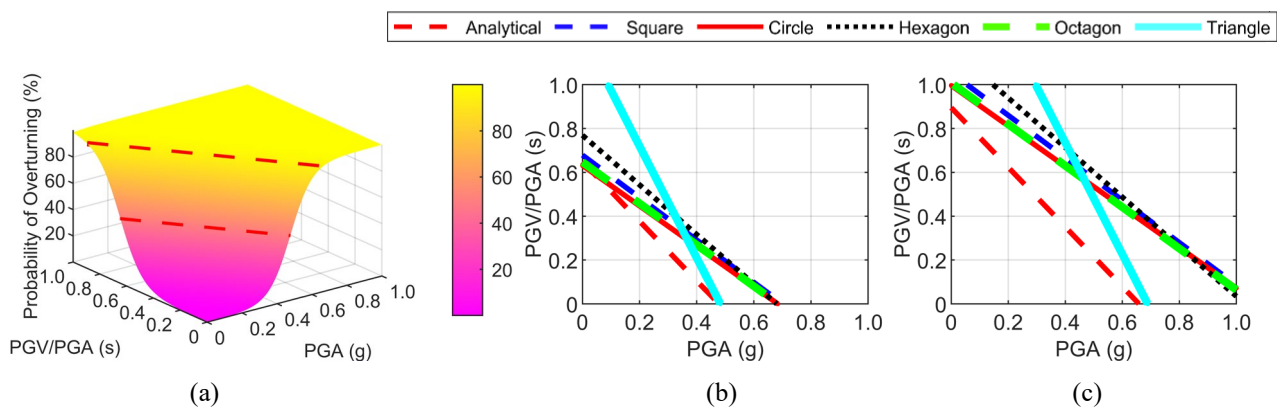


Fig. 9 – Analytical response a) Fragility Surface b) Comparison with experimental results at 50% probability level c) Comparison with experimental results at 95% probability level

5. Conclusion

In an effort to better predict the performance of freestanding structures under earthquake loads, this study evaluated the impact of the interface geometry on the overturning rates for freestanding structures through a preliminary numerical study followed by a detailed scaled shake table testing program. The preliminary



numerical study involved a realistic freestanding structure with arbitrary geometry for both the superstructure and the interface. When cast in a probabilistic formulation, the rate of overturning was substantially different when the interface geometry of the structure was increased arbitrarily by 10%. In order to more carefully study this problem, a shake table testing campaign was carried out for a freestanding structure including square, circular, hexagonal, octagonal, and triangular interfaces, where all critical rocking parameters were maintained. While the probabilities of overturning were fairly similar for most shapes (i.e., within 10%), the probabilistic responses were still different and highlight the need to carefully capture the interface geometry. In particular, the triangular base was substantially different in its rate of overturning with differences on the order of 40% for similar intensity earthquakes. This was mostly attributed to the unique response modes of the triangular base which typically incorporated point uplift, compared to edge uplift. In conclusion, the shape of the interface is noted to be a critical parameter when predicting the seismic response of freestanding structures; however, the theoretical or analytical equations of motion appear to yield conservative estimates for the simple geometries included in this study.

6. Acknowledgements

This study was partially supported by the United States Geological Survey through the Southern California Earthquake Center Award #19113 and Pacific Gas & Electric Company. The 3D printing of the structural models was partially supported by a Core Facility New User Grant for the Nano-Engineering Research Core Facility (NERCF), which receives funding from the Nebraska Research Initiative. The analytical and numerical simulations presented in this paper were completed utilizing the Holland Computer Center of the University of Nebraska, which receives support from the Nebraska Research Initiative. The second author was supported by the McNair Scholars Program at University of Nebraska-Lincoln, USA.

7. References

- [1] Milne J (1885): Seismic experiments. *Transactions of the Seismological Society of Japan*, **8**, 1–82.
- [2] Kirkpatrick P (1927): Seismic measurements by the overthrow of columns. *Bulletin of the Seismological Society of America*, **17** (2), 95–109.
- [3] Housner GW (1963): The behaviour of inverted pendulum structures during earthquakes. *Bulletin of the Seismological Society of America*, **53** (2), 403–417.
- [4] Ishiyama Y (1982): Motions of rigid bodies and criteria for overturning by earthquake excitations. *Earthquake Engineering & Structural Dynamics*, **10** (5), 635–650.
- [5] Shenton HW, Jones NP (1991): Base Excitation of Rigid Bodies. I: Formulation. *Journal of Engineering Mechanics*, **117** (10), 2286–2306.
- [6] Psycharis, IN (1990): Dynamic behaviour of rocking two-block assemblies. *Earthquake Engineering & Structural Dynamics*, **19** (4), 555–575.
- [7] Makris N, Roussos Y (2000): Rocking response of rigid blocks under near-source ground motions. *Geotechnique* **50** (3), 243–262.
- [8] Papantonopoulos C, Psycharis IN, Papastamatiou, DY, Lemos JV, Mouzakis HP (2002): Numerical prediction of the earthquake response of classical columns using the distinct element method, *Earthquake Engineering & Structural Dynamics*, **31** (9), 1699–1717.
- [9] Psycharis IN, Lemos JV, Papastamatiou DY, Zambas C, Papantonopoulos C (2003): Numerical study of the seismic behaviour of a part of the Parthenon Pronaos, *Earthquake Engineering & Structural Dynamics*, **32** (13), 2063–2084.
- [10] Peña F, Prieto F, Lourenço PB, Costa AC, Lemos JV (2007): On the dynamics of rocking motion of single rigid-block structures, *Earthquake Engineering & Structural Dynamics* **36** (15), 2383–2399.



- [11] Purvance MD (2005): *Overtuning of slender blocks: numerical investigation and application to precariously balanced rocks in southern California*, Ph.D. Dissertation, Department of Geological Sciences, University of Nevada, Reno, Nevada.
- [12] Purvance MD, Anooshehpour A, Brune JN (2008): Freestanding block overturning fragilities: Numerical simulation and experimental validation, *Earthquake Engineering & Structural Dynamics*, **37** (5), 791–808.
- [13] Wittich CE, Hutchinson, TC (2015): Shake table tests of stiff, unattached, asymmetric structures. *Earthquake Engineering & Structural Dynamics*, **44** (14), 2425–2443.
- [14] Wittich CE, Hutchinson TC (2017): Shake table tests of unattached, asymmetric, dual-body systems, *Earthquake Engineering & Structural Dynamics*, **46** (9), 1391-1410.
- [15] Mathey C, Feau C, Politopoulos I, Clair D, Baillet L, Fogli M (2016): Behavior of rigid blocks with geometrical defects under seismic motion: an experimental and numerical study. *Earthquake Engineering & Structural Dynamics*, **45** (15), 2455–2474.
- [16] Wittich CE, Hutchinson, TC (2018): Rocking bodies with arbitrary interface defects: Analytical development and experimental verification. *Earthquake Engineering & Structural Dynamics*, **47** (1), 69–85.
- [17] Bachmann JA (2018): *Development of self-centering Systems with geometry-controlled stiffness for earthquake hazard mitigation*, Ph.D. Dissertation, ETH Zurich, Zurich, Switzerland.
- [18] Makris N, Black CJ (2001): Rocking response of equipment anchored to a base foundation. *Technical Report PEER 2001/14*, Pacific Earthquake Engineering Research Center, University of California, Berkeley, USA.
- [19] Elgawady MA, Ma Q, Butterworth JW, Ingham J (2011): Effects of interface material on the performance of free rocking blocks. *Earthquake Engineering & Structural Dynamics*, **40** (4), 375–392.
- [20] Saifullah MK, Wittich CE (2019): Post-Earthquake Assessment and Numerical Modeling of Freestanding Heritage Structures. *12th Canadian Conference on Earthquake Engineering*, Quebec City, Quebec, Canada.
- [21] Kazhdan M, Bolitho M, Hoppe H, (2006): Poisson surface reconstruction. *Proc. 4th Eurographics Symposium on Geometry Processing*, Eurographics Association, Aire-la-Ville, Switzerland, 61–70.
- [22] Cignoni P, Callieri M, Corsini M, Dellepiane M, Ganovelli F, Ranzuglia G (2008): MeshLab: an open-source mesh processing tool. *Eurographics Italian Chapter Conference*, The Eurographics Association, 129–136.
- [23] Wittich CE, Hutchinson TC, Wood RL, Seracini M, Kuester F (2016) Characterization of Full-Scale, Human-Form, Culturally Important Statues: Case Study, *Journal of Computing in Civil Engineering*, **30** (3), 05015001.
- [24] D’Altri AM, Milani G, de Miranda S, Castellazzi G, Sarhosis V (2019): On the Stability Analysis of a Geometrically Complex Leaning Historic Structure in *Structural Analysis of Historical Constructions*, Springer (RILEM Bookseries), vol 18.
- [25] Itasca Consulting Group, Inc. (2016): *3DEC — Three-Dimensional Distinct Element Code*, Ver. 5.2. Minneapolis, Itasca.
- [26] Cundall PA, Strack ODL (1979): A discrete numerical model for granular assemblies. *Géotechnique*, **29** (1), 47–65.
- [27] Ancheta TD, Darragh RB, Stewart JP, Seyhan E, Silva WJ, Chiou BSJ, Wooddell KE, Graves RW, Kottke AR, Boore DM, Kishida T, Donahue JL (2013): PEER NGA-West2 Database. Technical Report PEER 2013/03, Pacific Earthquake Engineering Research, Berkeley, USA.
- [28] Center for Engineering Strong Motion Data (2015): Lamjung, Nepal Earthquake of 25 April 2015, CESMD. Retrieved from: <<https://strongmotioncenter.org>>
- [29] Boore, DM (2010): Orientation-Independent, Nongeometric-Mean Measures of Seismic Intensity from Two Horizontal Components of Motion. *Bulletin of the Seismological Society of America*, **100** (4), 1830–1835.
- [30] The MathWorks, Inc. (2019): MATLAB 9.6. Natick, Massachusetts, USA.